Altered ECM deposition by diabetic foot ulcer-derived fibroblasts implicates fibronectin in chronic wound repair

Anna G. Maione, PhD[1]; Avi Smith, BA[1]; Olga Kashpur, PhD[1]; Vanessa Yanez, BS[1]; Elana Knight, BS[1]; David J. Mooney, PhD[2,3]; Aristidis Veves, MD, DSc[4]; Marjana Tomic-Canic, PhD[5]; Jonathan A. Garlick, PhD, DDS[1]

1. Department of Oral and Maxillofacial Pathology, Oral Medicine and Craniofacial Pain, Tufts University School of Dental Medicine, Boston, Massachusetts,
2. Wyss Institute for Biologically Inspired Engineering, Harvard University, Boston, Massachusetts,
3. School of Engineering and Applied Sciences, Harvard University, Cambridge, Massachusetts,
4. Microcirculation Laboratory and Joslin-Beth Israel Deaconess Foot Center, Beth Israel Deaconess Medical Center, Harvard Medical School, Boston, Massachusetts,
5. Department of Dermatology & Cutaneous Surgery, Wound Healing and Regenerative Medicine Research Program, University of Miami Miller Medical School, Miami, Florida

Reprint requests:
Dr. Jonathan A. Garlick, PhD, DDS, Department of Oral and Maxillofacial Pathology, Oral Medicine and Craniofacial Pain School of Dental Medicine Tufts University 55 Kneeland St., South Cove, Room 116 Boston, MA 02111, USA.
Tel: 617-636-2478;
Fax: 617-636-2915;
Email: jonathan.garlick@tufts.edu

Manuscript received: November 2, 2015
Accepted in final form: April 19, 2016

DOI:10.1111/wrr.12437

ABSTRACT

Current chronic wound treatments often fail to promote healing of diabetic foot ulcers (DFU), leading to amputation and increased patient morbidity. A critical mediator of proper wound healing is the production, assembly, and remodeling of the extracellular matrix (ECM) by fibroblasts. However, little is known about how these processes are altered in fibroblasts within the DFU microenvironment. Thus, we investigated the capacity of multiple, primary DFU-derived fibroblast strains to express, produce, and assemble ECM proteins compared to diabetic patient-derived fibroblasts and healthy donor-derived fibroblasts. Gene expression microarray analysis showed differential expression of ECM and ECM-regulatory genes by DFU-derived fibroblasts which translated to functional differences in a 3D in vitro ECM tissue model. DFU-derived fibroblasts produced thin, fibronectin-rich matrices, and responded abnormally when challenged with transforming growth factor-beta, a key regulator of matrix production during healing. These results provide novel evidence that DFU-derived fibroblasts contribute to the defective matrices of DFUs and chronic wound pathogenesis.

INTRODUCTION

Diabetic foot ulcers (DFU) significantly impair patient quality of life and lead to prolonged hospitalizations. These chronic wounds have been linked to altered production of extracellular matrix (ECM) proteins,[1–6] aberrant cellular infiltration,[7] and compromised angiogenesis.[8,9] Although understanding of the pathophysiology of DFUs has increased in recent years,[2,10,11] existing therapies continue to have high failure rates and require repeat applications that drive up treatment costs.[12–15] Thus, there is a compelling need to better understand the biological basis of DFUs to develop more effective therapies.[16]

DFUs develop when one or more of the spatially and temporally coordinated processes in the wound healing cascade go awry. One of the critical mediators of cutaneous wound healing is the ECM. During the early, proliferative phase of physiologic wound healing, a provisional ECM, consisting of fibronectin, tenascin, and Type III Collagen is secreted and assembled by fibroblasts. This provisional matrix serves as a scaffold for cell migration and proliferation, and as a depot for growth factor release.[12–14] During the subsequent remodeling phase of healing, Type I Collagen replaces fibronectin, becoming the predominant ECM constituent and resulting in a more mature ECM. Despite our understanding of the role of fibronectin in physiological wound healing, its involvement in the impaired healing of DFUs remains unclear.

While altered ECM production has been implicated in the impaired healing of chronic wounds,[4,6,15,17] the nature of these alterations varies between studies. For instance, it has been shown that venous ulcer-derived fibroblasts synthesize similar amounts of fibronectin in vitro when compared to healthy fibroblasts. Yet, immunohistological studies have shown that the base of venous ulcers is deficient in fibronectin.[18] Unlike in venous ulcers, fibronectin expression is known to be elevated in a variety of organs

3D	Three-dimensional
COL1	Type I Collagen
DAPI	4′,6-diamidino-2-phenylindole
DFU	Diabetic foot ulcer
ECM	Extracellular matrix
Fn	Fibronectin
H&E	Hematoxylin and eosin
TGF-β	Transforming growth factor-beta

www.manaraa.com

associated with diabetic complications,[19] however the biological significance of elevated fibronectin in diabetic skin wounds has not been established. It has been suggested that sustained expression, incomplete degradation, and/or inadequate clearance of fibronectin prevents the shift from the proliferative to remodeling phase and limits cutaneous wound healing.[5] In contrast, it has been shown that topical application of fibronectin may improve wound healing in diabetic mice.[4,18] Further studies are needed to elucidate how fibronectin participates in the impaired healing microenvironment of DFUs.

One of the primary mediators of ECM production and remodeling is transforming growth factor-beta (TGF-β). During physiological wound healing, latent TGF-β is sequestered in the ECM. When activated, TGF-β stimulates fibroblast proliferation and differentiation into myofibroblasts, which secrete, remodel, and contract the ECM.[17] Therefore, the altered response of fibroblasts to TGF-β in chronic wounds could play an integral role in impaired ECM deposition and reorganization.

To more accurately study how an altered ECM contributes to impaired DFU healing, we recently developed a three-dimensional (3D) tissue model that closely mimics the in vivo diabetic ECM microenvironment.[20] In this model, primary human fibroblasts are stimulated to secrete and assemble a 3D ECM tissue that is similar in composition to wound granulation tissue.[21] In the current study, we used this platform to demonstrate that fibroblasts isolated from DFUs (DFUFs) and site-matched, nonulcerated, diabetic skin (DFFs) produced significantly less ECM compared to those isolated from site-matched, nonulcerated, nondiabetic skin (NFFs).[20] In spite of this, DFUF-produced ECM tissues exhibited higher levels of fibronectin, similar to what is known to occur in diabetic kidney disease.[19] This elevated expression of fibronectin suggests that DFU-derived fibroblasts in 3D tissues models retain properties of the in vivo diabetic microenvironment. When challenged with TGF-β, DFUFs produced 3D ECM tissues that were morphologically similar to DFFs and NFFs, suggesting that reduced ECM production and failure to heal may not be due to the inability of DFU fibroblasts to respond to TGF-β. However, the fibronectin content was reduced in TGF-β-stimulated matrices produced by DFUFs compared to those produced by DFFs and NFFs. This suggests that while DFUFs are responsive to TGF-β, their response is atypical and may contribute to impaired ulcer healing.

METHODS

Cell culture

Primary fibroblasts were isolated from discarded, de-identified skin specimens collected under a protocol approved by the Beth Israel Deaconess Medical Center Institutional Review Board. Three groups of fibroblasts were isolated, all from different patients: diabetic foot ulcer-derived fibroblasts (DFUF), nonulcerated, site-matched, diabetic foot fibroblasts (DFF), and nonulcerated, site-matched nondiabetic foot fibroblasts (NFF). All fibroblasts were expanded and maintained in fibroblast growth media consisting of DMEM (Invitrogen, Carlsbad, CA), 10% FBS (HyClone, Logan, UT), HEPES (Sigma-Aldrich, St. Louis, MO), and Pen/Strep/Fung (Invitrogen) at 37°C and 7.5% CO_2. Fibroblasts were passaged when confluent using 0.05% trypsin/EDTA (Invitrogen). Experiments were conducted with cells between passages 4 and 7.

Gene expression microarray

The Illumina HumanHT-12 v4 Expression BeadChip array containing more than 47,000 probes was used to investigate genome-wide transcriptional expression differences between fibroblast groups (Illumina, San Diego, CA). Briefly, fibroblasts were grown until confluence and RNA was isolated using a Qiagen RNeasy Mini kit according to manufacturer's instructions (Qiagen, Hilden, Germany). RNA quality and purity were confirmed using a nanodrop (Thermo Scientific, Waltham, MA) and bioanalyzer (Agilent, Santa Clara, CA). Samples with an RNA Integrity Number (RIN) of 9 or greater were used. The Yale Center for Genome Analysis (New Haven, CT) performed hybridization of the samples and scanning of the array according to the manufacturer's instructions. Raw data was analyzed using R/Bioconducter and MicroarrayRUs.[22,23] Quality control analyses indicated that all arrays were of high quality with no technical outliers. Data were then log transformed and quantile normalized. Differentially expressed genes were determined using the limma implementation of 1-way ANOVA with 1.5-fold change and p-value ≤ 0.05 cutoffs. GOrilla was used to perform gene set enrichment analysis.[24]

Immunofluorescence

To examine the localization of Type I Collagen and fibronectin, immunofluorescence staining was performed on fibroblasts grown in monolayer culture by standard staining procedures. Briefly, fibroblasts were grown on chamber slides and fixed with 4% paraformaldehyde for five minutes. Cells were blocked in 5% goat serum/0.2% BSA/PBS with and without permeabilization with 0.1% Triton-X for 30 min at room temperature. Then, cells were incubated in primary antibody in 0.2% BSA/PBS for 1 hour at room temperature, washed, and incubated in appropriate secondary antibodies (Invitrogen). Slides were mounted with DAPI (Vector Labs, Burlingame, CA) and imaged using a Nikon Eclipse 80i microscope and Spot Advanced software (Diagnostic Instruments, Sterling Heights, MI). Primary antibodies used were anti-Collagen Type I (Abcam, Cambridge, MA) and anti-Fibronectin (BD Biosciences, San Jose, CA).

Fabrication of 3D self-assembled ECM tissues cultures

Using a 3D self-assembled ECM model previously established in our lab,[20,21] we measured differences in the capacity of the fibroblasts to produce an ECM that is similar to granulation tissue during normal wound repair. Fibroblasts were seeded in six replicate wells (three for histology and three for protein collection) in 1.0 μM pore Millicell Hanging Cell Culture inserts (Millipore, Billerica, MA), at a density of 5×10^5 cells/cm^2. Cells were fed every 3 days with media supplemented with 10 μg/mL ascorbic acid (Sigma-Aldrich). After 5 weeks, three tissues

www.manaraa.com

were frozen in liquid nitrogen for later protein extraction. The remaining three tissues were fixed with 10% buffered formalin overnight, processed, paraffin-embedded, and tissue sections were stained by hematoxylin and eosin (H&E). To measure ECM production, three random areas of multiple tissue sections were used to quantify the tissue area normalized to section length and cell number using ImageJ software (NIH, Bethesda, MD). Tissue thickness is expressed as mean thickness μM/cell ± S.D. For TGF-β stimulation of ECM tissues, 2 ng/mL TGF-β1 (R&D Systems, Minneapolis, MN) were added to the media for the final 2 weeks of culture. To capture tissue morphology, the entire tissue length was imaged and the images were compiled into a panorama using Image Composite Editor (Microsoft, Redmond, WA).

Protein extraction and Western blot

To examine the composition of ECM tissues, protein was extracted from three, pooled replicate tissues grown in the 3D self-assembly assay. Deoxycholate (Sigma-Aldrich) lysis buffer with protease inhibitors was added to the tissues[21] and tissues were homogenized by hand using a plastic pestle. Homogenates were then sonicated briefly three times on ice. Protein concentration was determined using a BCA protein assay (ThermoFisher Scientific, Pierce, Rockford, IL).

For Western blot analysis, protein samples were separated on a 4–20% SDS-PAGE pre-cast gel (Bio-Rad, Hercules, CA) and transferred to a nitrocellulose membrane. Membranes were blocked in 5% milk/PBST for 1 hour at room temperature and then incubated in primary antibody in 5% milk/PBST overnight at 4 °C (Fibronectin; BD Biosciences, GAPDH; Abcam, Type I Collagen; Abcam, EDA-containing fibronectin; Abcam). The following day, membranes were washed with PBST and incubated in appropriate secondary antibody (Jackson ImmunoResearch Laboratories, Inc.) at a concentration of 1:10,000 in 5% milk/PBST for 1 hour at room temperature. The blots for fibronectin, Type I Collagen, and GAPDH from the 12 fibroblast strains were developed using Clarity Western ECL (Bio-Rad) and x-ray radiography film. Densitometry was performed using ImageJ and expression was normalized to GAPDH. All other blots were imaged using Bio-Rad's ChemiDoc MP imaging system and were normalized to total protein. Blots were repeated at least twice and images and quantification shown are representative results.

Collagen gel contraction assay

To assess the ability of fibroblasts to contract and remodel a matrix in response to TGF-β, a floating collagen gel contraction assay was performed similarly to established protocols.[25] Fibroblasts were mixed with PureCol bovine Type I Collagen solution (Advanced BioMatrix, San Diego, CA, final concentration 1.5 mg/mL) on ice and plated in a 24-well culture plate. Gels were allowed to solidify at 37 °C for one hour, at which point 0.1% serum media was added on top of the gels. The following day, the gels were carefully detached from the edges of each well and stimulated with vehicle or 2 ng/mL TGF-β1 (R&D Systems) in 0.1% serum media for 5 days. The gels were imaged with a digital camera (Fujifilm, Valhalla, NY) and the surface area was quantified using ImageJ. Gel contraction is expressed as mean ± S.D percent decrease in surface area relative to vehicle control treatment of triplicate gels.

RNA extraction

Total RNA was extracted from DFUF, DFF, and NFF fibroblasts grown in monolayer at passage 4 using the Qiagen RNeasy mini kit following the manufacturer's instructions. RNA quality was assessed using a bioanalyzer (Agilent technologies) to estimate the RNA integrity number. Samples with a RIN higher than 5 were used.

Analysis of gene expression by qRT-PCR

For gene expression analysis, cDNA was made with iScript cDNA Synthesis kit (Bio-Rad). One nanogram of RNA was used per reverse transcription reaction. All real-time PCR reactions were done in triplicate using the iQ SYBR Green SuperMix (Bio-Rad) and the relative gene expression was calculated using the ddCt method. GAPDH was used as a reference gene. Sequences of primers used in qRT-PCR are presented in Supporting Information Table S1. ACTA2 primers were purchased from Bio-Rad (Cat# 10025636).

Statistics

All results are expressed as mean ± S.D. of at least three independent samples. Statistical analyses were performed using IBM SPSS. One-way ANOVA and appropriate post-hoc tests (Tukey's HSD or Games-Howell) determined statistical significance. $*p \leq 0.05$ and $**p \leq 0.01$ were considered significant.

RESULTS

DFUFs and DFFs displayed differential gene expression profiles when compared to NFFs by microarray analysis

Before using patient derived primary fibroblast cell lines in 3D tissue experiments, it was important to determine if they retained distinct patterns of gene expression that reflected their in vivo tissue microenvironment after expansion in monolayer culture. First, we established twelve, site-matched, primary fibroblast cultures from patient biopsies that were categorized into three groups: DFUFs, DFFs (nonulcerated, diabetic foot fibroblasts), and NFFs (nonulcerated, nondiabetic foot fibroblasts). We performed gene expression microarray analysis on these twelve cell strains using Illumina's human BeadChip array and conducted unsupervised hierarchal clustering using Euclidian distance and Ward linkage to determine global patterns in mRNA expression. The resulting dendrogram identified two main branches; one primarily containing fibroblasts derived from diabetic patients (DFUFs and DFFs) and the other, primarily containing control NFFs. This indicated that DFUFs and DFFs were more similar to each other than to NFFs after isolation and expansion in monolayer culture (Figure 1a). While one fibroblast strain per group did not follow this pattern, the overall trend indicates that, despite patient variability, differences in

www.manaraa.com

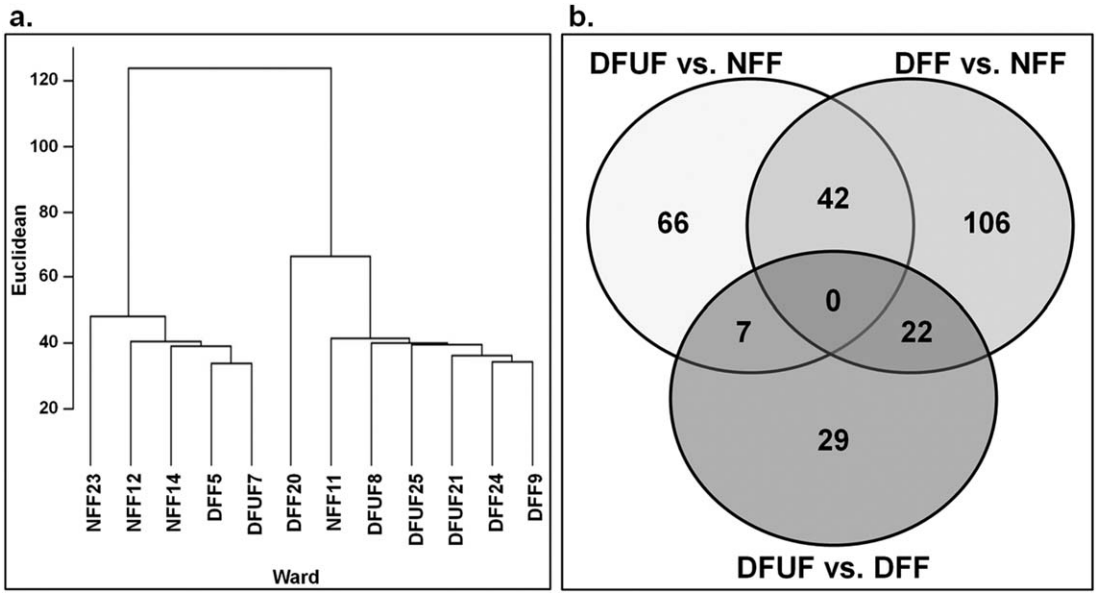

Figure 1. Microarray analysis revealed distinct gene expression profiles of diabetic patient-derived fibroblasts. (a) Hierarchical cluster analysis showed two separate branches; one containing the majority of the DFUFs and DFFs, the other containing the majority of NFFs, indicating distinct global gene expression profiles based on diabetic origin. (b) A Venn diagram representing the number of differentially expressed genes ($\geq$1.5-fold change, $p \leq 0.05$) further confirmed that DFUFs and DFFs were more similar to each other than either compared to the NFFs.

gene expression linked to the diabetic environment are detectable after expansion in monolayer culture. This indicated that primary diabetic and nondiabetic cell lines are representative of their in vivo environment and would be suitable for further analyses.

Differentially expressed gene (DEG) lists were generated using the 1-way ANOVA implementation in the limma package of Bioconductor.[22] DEG lists were then filtered to include only fold change differences greater than 1.5 and *p*-values less than 0.05. This analysis identified 170 differentially expressed genes between DFFs and NFFs, 115 differentially expressed genes between DFUFs and NFFs, and 58 differentially expressed genes between DFUFs and DFFs. The number of overlapping genes between DEG lists is shown in a Venn diagram (Figure 1b). Differentially expressed gene lists are provided in Supporting Information Tables S2–S4. These results support the cluster analysis findings by confirming that fewer genes were differentially expressed between DFUFs and DFFs compared to DFUFs vs. NFFs and DFFs vs. NFFs. Importantly, this suggests that cultured, primary fibroblasts retain a "memory" of their in vivo origin, as we have previously shown through whole genome methylation analysis.[26]

Analysis of differentially expressed genes revealed enrichment in ECM-related gene terms

To determine processes, functions, and cellular components that were represented in the DEG lists, gene set enrichment analysis was conducted. Enrichment in gene ontology terms related to glucose metabolism supported that microarray analysis detected differences between fibroblast groups based on diabetes status (Table 1). Additionally, we found that processes related to wound healing, such as leukocyte chemotaxis, cell migration, cytokine production, and angiogenesis, were also enriched. These results suggest that several critical wound healing-related processes may be altered in DFUFs and DFFs when compared to healthy, site-matched NFFs. Interestingly, several gene terms pertaining to ECM production and organization were significantly enriched in each of the three categories; biological processes, molecular functions, and cellular components (Table 1). Since the deposition and assembly of a provisional matrix and its reorganization into a mature ECM are essential functions of fibroblasts during wound healing, we sought to determine how these gene expression differences translated into functional differences.

DFUFs and DFFs Show altered secretion of Type I Collagen into the extracellular space

Based on the microarray finding that ECM genes, particularly several collagen genes, were differentially expressed between DFUFs and NFFs, we examined expression and localization of Type I Collagen, the principal component of the dermal ECM. Immunofluorescent staining following permeabilization of fibroblasts grown in monolayer revealed that Type I Collagen produced by all DFUF and DFF strains remained predominantly intracellular, as distinct cell boundaries could be clearly identified (Figure 2). However, three out of the four NFF cell strains exported the collagen into the extracellular space, as suggested by the diffuse, mesh-like staining pattern (Figure 2). Interestingly, the NFF11 cell line exhibited intracellular staining for Type I Collagen, similar to the DFUFs and DFFs, and it also

www.manaraa.com

Table 1. Gene set enrichment analysis of differentially expressed genes

GO term	Description	*p*-Value	FDR *q*-value	Enrichment score
Biological process				
GO:0019682	Glyceraldehyde-3-phosphate metabolic process	3.70 E −04	3.23 E −02	59.62
GO:2000353	Positive regulation of endothelial cell apoptotic process	2.13 E −04	2.30 E −02	24.39
GO:0002686	Negative regulation of leukocyte migration	5.15 E −05	9.66 E −03	18.83
GO:0048247	Lymphocyte chemotaxis	6.92 E −04	4.99 E −02	16.77
GO:0006096	Glycolytic process and gluconeogenesis	4.50 E −07	4.41 E −04	14.56
GO:0050710	Negative regulation of cytokine secretion	3.31 E −04	3.08 E −02	11.92
GO:0030199	Collagen fibril organization	7.95 E −05	1.30 E −02	11.18
GO:0032963	Collagen metabolic process	3.98 E −05	7.92 E −03	7.54
GO:0030336	Negative regulation of cell migration	1.37 E −05	3.70 E −03	5.56
GO:0006006	Glucose metabolic process	3.93 E −05	7.95 E −03	5.51
GO:0030198	Extracellular matrix organization and assembly	6.57 E −10	8.37 E −06	5.23
GO:0045765	Regulation of angiogenesis	1.73 E −04	1.97 E −02	4.55
GO:0060429	Epithelium development	5.58 E −04	4.25 E −02	3.55
GO:0008283	Cell proliferation	6.05 E −05	1.09 E −02	2.77
Molecular function				
GO:0001968	Fibronectin binding	7.36 E −06	3.00 E −02	17.89
GO:0005201	Extracellular matrix structural constituent	1.07 E −05	2.18 E −02	9.21
Cellular component				
GO:0005604	Basement membrane	1.57 E −05	2.29 E −03	8.70
GO:0044420	Extracellular matrix part	1.34 E −07	2.45 E −05	8.00
GO:0005581	Collagen trimer	5.80 E −05	7.73 E −03	7.11
GO:0031012	Extracellular matrix	2.66 E −07	4.33 E −05	4.50

clustered with the DFUFs and DFFs in the hierarchical cluster analysis (Figure 1a). Immunofluorescent staining without permeabilization showed a punctate pattern suggestive of extracellular Type I Collagen localization in DFUFs and DFFs. In contrast, NFFs showed a mesh-like staining pattern in the extracellular space (Figure 3). These data indicate that Type I Collagen is found predominantly in an intracellular location in DFUFs and DFFs when compared to NFFs, which export all of their Type I Collagen into extracellular space. This different staining pattern was revealed when cell cultures were stained with and without or without permeabilization. Treatment of fibroblast monolayers with TGF-β, a key mediator of wound healing and collagen production, resulted in increased production of Type I Collagen by all cell lines. The same pattern of Type I Collagen staining was observed with TGF-β treatment as with vehicle control treatment, however, the amount of collagen produced by each fibroblast strain tended to increase (Figures 2 and 3). To determine that DFUFs remain responsive to TGF-β stimulation, we next treated monolayer cultures of all 12 lines with TGF-β, and assayed activation of alpha smooth muscle actin (ACTA2), a known target gene of the TGF-β pathway. We found that ACTA2 was upregulated in response to TGF-β treatment in all 12 fibroblast lines, indicating that NFFs, DFFs and DFUFs are responsive to TGF-β stimulation (Figure 4). These observations suggest that fibroblasts derived from diabetic patients may be limited in their export and/or extracellular assembly of collagen, in spite of being responsive to TGF-β.

DFUFs secreted and assembled a thin ECM tissue enriched in fibronectin and Type I Collagen

While Type I Collagen is the primary constituent of a mature dermal ECM, fibronectin is the predominant ECM protein found in the provisional matrix during early wound healing and it provides a scaffold for subsequent collagen deposition. To examine fibronectin expression and localization, we stained DFUF, DFF, and NFF monolayers cultured with and without TGF-β. Unlike Type I Collagen, there was no difference in fibronectin localization between fibroblast types, although there was slightly less fibronectin expression in DFUFs compared to DFFs and NFFs (Supporting Information Figure S1). TGF-β treatment appeared to increase fibronectin production in all fibroblast cell strains, further supporting that DFUFs and DFFs are responsive to TGF-β.

To extend these results to a more physiologically relevant environment, we assessed the de novo ECM production and assembly of DFUFs, DFFs, and NFFs using a 3D ECM tissue model that mimics early wound granulation tissue.[21] DFUFs and DFFs produced thinner ECM tissues compared to NFFs (Figure 5a). Quantification of ECM thickness per cell showed that DFUFs and DFFs produced about twofold thinner matrices than NFFs (Figure 5b). These data further support the finding that ECM secretion and assembly is impaired in DFUFs and DFFs.

Gene expression analysis of fibroblasts cultured as monolayers and 3D ECM tissues also confirms that DFUFs and DFFs are impaired in ECM production (Figure 6).

www.manaraa.com

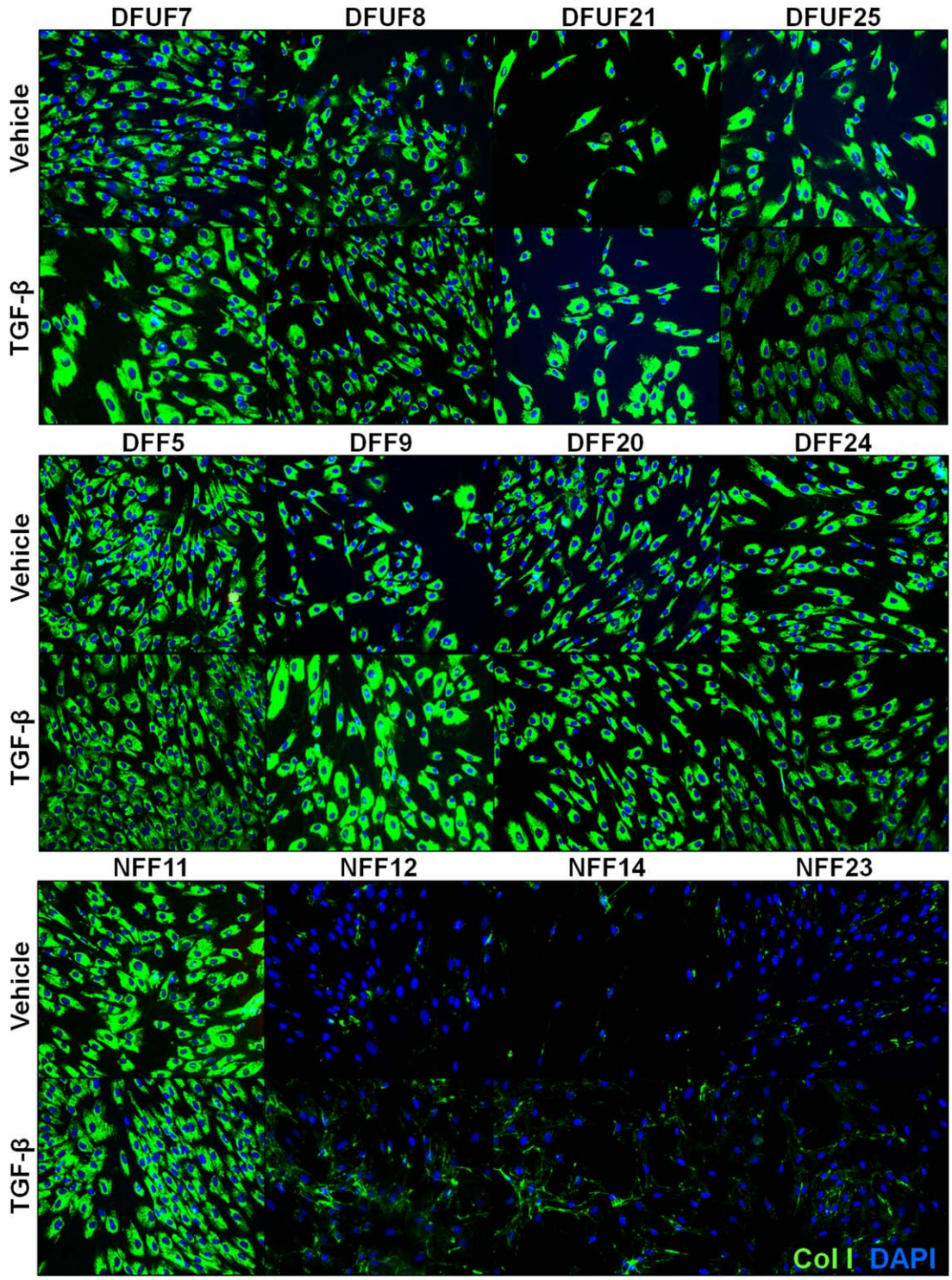

Figure 2. DFUFs and DFFs show predominantly intracellular Type I Collagen. Monolayers cultures of DFUFs, DFFs, and NFFs were treated for 48 hours with 2 ng/mL TGF-β or vehicle control and stained for Type I Collagen and DAPI. Immunofluorescent staining with permeabilization showed that DFUFs and DFFs exhibited predominantly intracellular staining for Type I Collagen, while three out of four NFFs exhibited an extracellular, mesh-like staining pattern.

www.manaraa.com

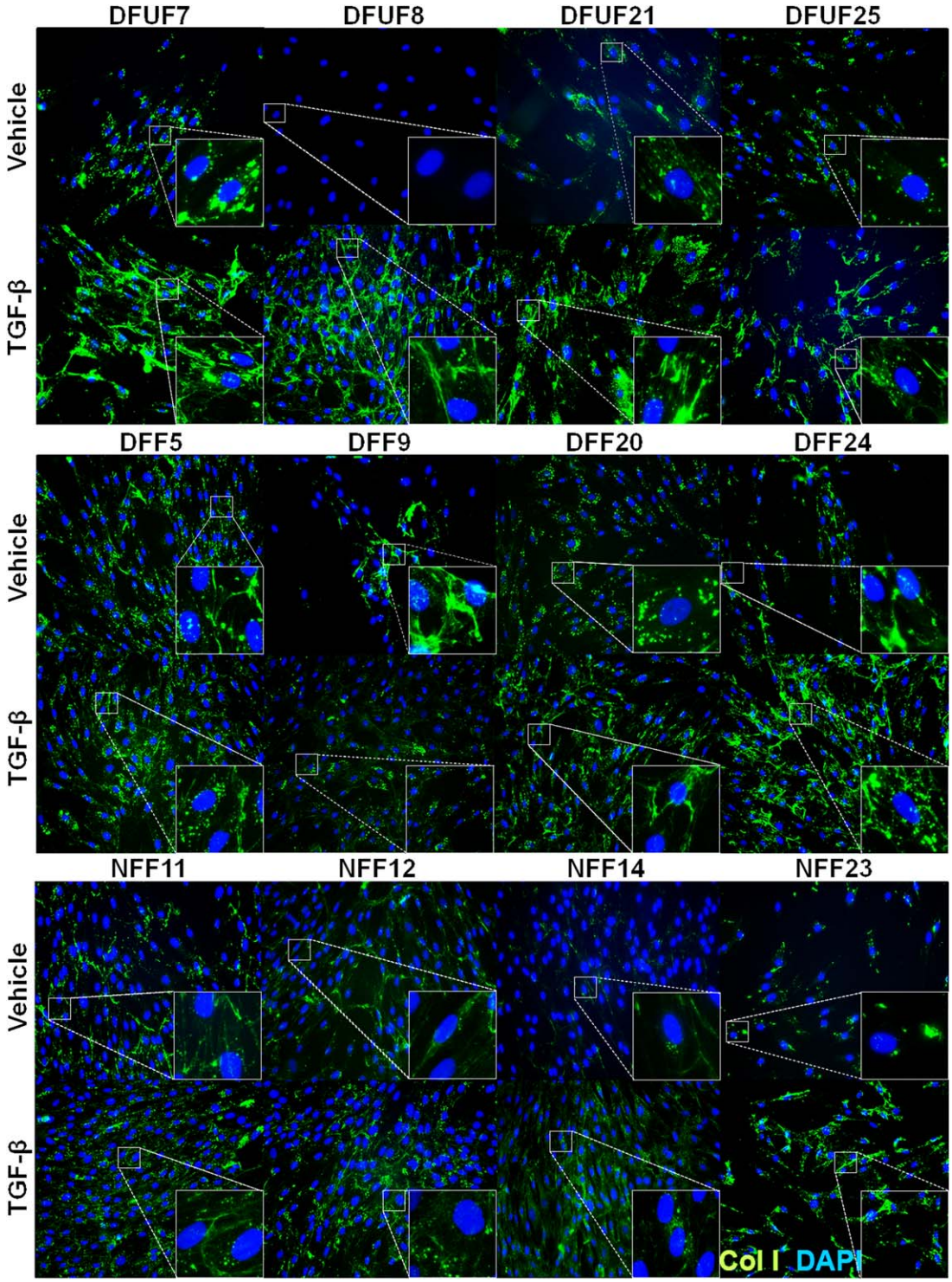

Figure 3. DFUFs and DFFs show altered pattern of Type I Collagen extracellular localization. Monolayer cultures of DFUFs, DFFs, and NFFs were treated for 48 hours with 2 ng/mL TGF-β or vehicle control and stained without permeabilization for Type I Collagen and DAPI. Inserts show 40× magnification.

www.manaraa.com

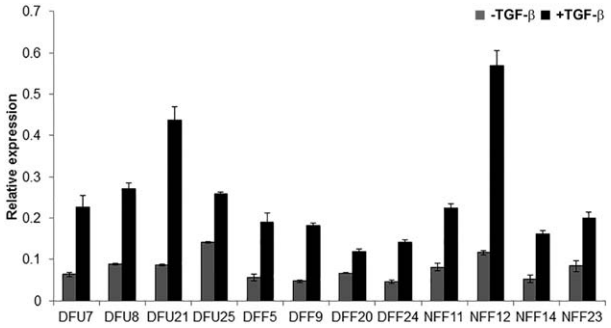

Figure 4. DFUFs, DFFs, and NFFs are responsive to TGF-β stimulation. DFUFs, DFFs and NFFs grown in monolayer were stimulated with 2 ng/ml of TGF-β. qRT-PCR analysis shows activation of alpha smooth muscle actin (ACTA2) in all 12 cell lines after TGF-β treatment.

qRT-PCR analysis showed that DFUFs and DFFs have lower levels of COL1A1 in monolayer (Figure 6a). This difference was not observed when fibroblasts were cultured in 3D, ECM tissues, where expression levels remained the same (Figure 6a). In contrast, expression levels of COl1A2 were similar in both monolayer culture and 3D ECM tissues for all DFUF, DFF and NFF cell lines (Figure 6b). Expression of Type IV Collagen (COL4A1) was elevated in NFFs in 3D ECM tissues, but there was no difference in the expression levels of Type IV Collagen (COL4A1) in 2D cultures (Figure 6c). Fibronectin expression was elevated in DFUFs and DFFs compared to NFFs in both monolayer culture and 3D ECM tissues (Figure 6d). This shows that gene expression changes evident in monolayer culture are maintained in 3D ECM tissues only for fibronectin. Differences in gene expression between monolayer and 3D ECM for Type I Collagen and Type IV Collagen show the importance of using 3D in vivo like

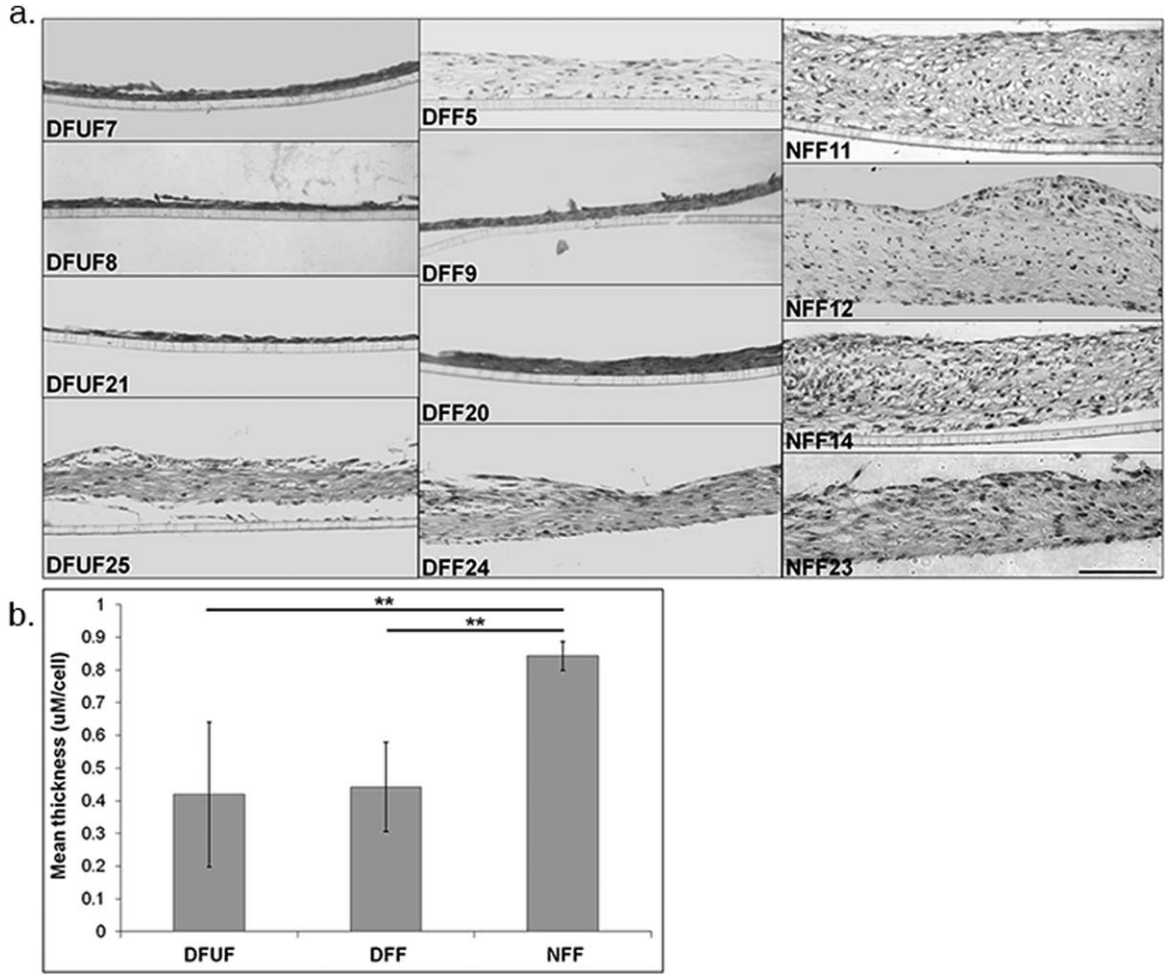

Figure 5. DFUFs and DFFs produced less ECM than NFFs in a 3D ECM tissue model. For 5 weeks, DFUFs, DFFs, and NFFs were stimulated with ascorbic acid to secrete and assemble an ECM. Representative H&E stained cross sections of the ECM tissues showed that DFUF- and DFF-produced matrices were significantly thinner than those produced by NFFs. Quantification of ECM thickness relative to cell number verified the decreased de novo production of ECM by DFUFs and DFFs. Scale bar, 100 μM. $^{**}p \leq 0.01$.

www.manaraa.com

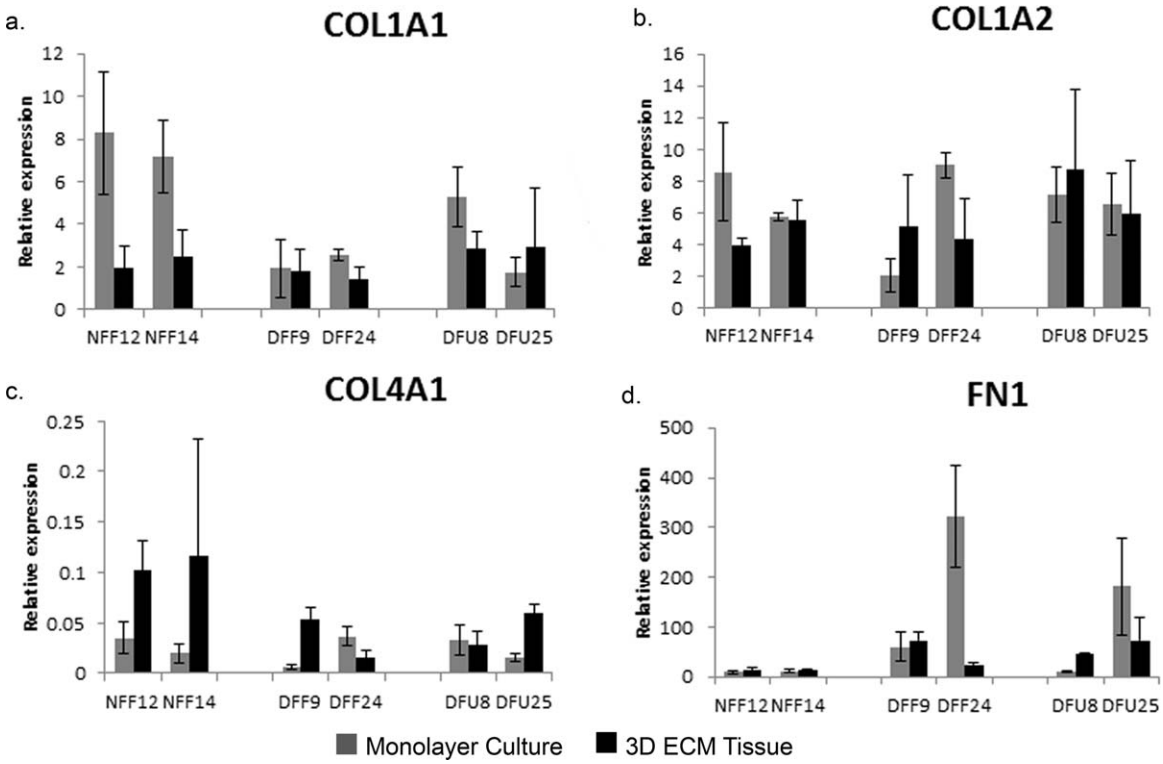

Figure 6. DFUFs, DFFs and NFFs show differences in gene expression between monolayer culture and 3D ECM tissues. qRT-PCR analysis of (a) COL1A1, (b) COL1A2, (c) COL4A1 and (d) FN1 expression normalized to GAPDH showed differences between cell lines and between monolayer culture and in vivo–like 3D ECM tissue models.

models when evaluating wound healing properties of fibroblasts in addition to monolayer culture.

Since fibronectin is known to be highly up-regulated in the early wound matrix and is elevated in diabetic tissues in vivo, we assessed fibronectin composition of the ECM tissues by Western blot. Although DFUFs producing thinner 3D tissues, they produced an average of threefold and fourfold more fibronectin than DFFs and NFFs, respectively (Figure 7a and b). These data are consistent with published findings that fibronectin expression is increased in diabetic patient skin and under hyperglycemic conditions.[6] Although DFUFs produce a thinner ECM, they produced more fibronectin in 3D ECM tissues. To determine if the increased thickness seen in NFFs could be accounted for by increased secretion of Type I Collagen, we assayed its production in 3D ECM tissues produced by DFUFs, DFFs, and NFFs. We found that DFUF, and DFFs produced more Type I Collagen than NFFs in our 3D ECM tissue model (Figure 7c and d). This suggests that additional ECM proteins other than Type I Collagen and fibronectin may be linked to the increased thickness seen in NFFs compared to DFUFs and DFFs. Together, these results show that DFU-derived fibroblasts have an altered ECM phenotype characterized by the elevated expression of Type I Collagen and fibronectin which may affect their ability to support normal wound repair.

DFUFs exhibited an aberrant response to TGF-β in 3D ECM tissues

Based on our finding that DFUFs increased ECM protein expression in response to TGF-β in monolayer cultures, we next determined if TGF-β could also augment DFUF matrix production in 3D self-assembled ECM tissues. Following two weeks of exposure to TGF-β, the ECM morphology was dramatically altered in tissues produced by all three fibroblast types; TGF-β-treated tissues were shorter and thicker than the long and thin, untreated tissues (Figure 8). These results further support our findings that DFUFs are capable of responding to TGF-β signaling.

We hypothesized that TGF-β could be causing the thickening of the tissues by promoting fibroblast contraction of the matrix, similar to its role in vivo.[17] Using a collagen gel contraction assay, we assessed the capacity of DFUFs, DFFs, and NFFs to contract and remodel a preformed collagen gel in response to TGF-β. In DFF- and NFF-populated gels, TGF-β treatment induced contraction as demonstrated by the 1.8- and 2-fold reduction in surface area, respectively (Supporting Information Figure S2). However, TGF-β treatment did not induce contraction in DFUF-populated gels compared to vehicle treatment. While previous results showed that DFUFs are responsive to TGF-β, these data indicate that their contractile response is defective when compared to DFFs and NFFs.

Since DFUFs produced fibronectin-rich ECM tissues compared to DFFs and NFFs and TGF-β is known to up-regulate fibronectin production, we investigated the expression of fibronectin in 3D ECM tissues following TGF-β stimulation. In all DFF-produced matrices and

www.manaraa.com

three of four NFF-produced matrices, fibronectin content was greater in the TGF-β-treated tissues compared to untreated tissues (Figure 9a). Conversely, fibronectin content in three of four DFUF-produced matrices was less in TGF-β-treated matrices compared to untreated controls. These results were confirmed by densitometric quantification of the Western blots normalized to total protein loaded (Figure 9b). The decreased fibronectin content could indicate that DFUFs are less able to produce a healthy granulation tissue in response to TGF-β in the chronic wound environment.

TGF-β is also known to stimulate expression of an alternatively spliced fibronectin isoform which contains Type III Extra domain A. In order to determine if there are differences in alternatively spliced isoforms of fibronectin produced by DFUFs, DFF and NFFs in 3D ECM tissue, we assessed expression of EDA-containing fibronectin by Western blot. We found that expression of this alternatively spliced fibronectin isoform (EDA-containing fibronectin) was similar in DFUFs, DFF and NFFs in 3D ECM tissue (Figure 9c). Fibroblasts from all donor sources respond to TGF-β stimulation by generating shorter and thicker ECM in 3D ECM tissues (Figure 8), however DFUFs produce less fibronectin when stimulated with TGF-β (Figure 9a and b). In order to further understand the molecular reason for this TGF-β-mediated morphological transformation, we tested expression of the alternatively spliced isoform EDA-containing fibronectin in 3D ECM tissues stimulated with TGF-β. Western blot analysis showed that EDA-containing fibronectin was up-regulated by TGF-β treatment in three out of four NFFs and all DFFs. Three out of four DFUFs did not show greater content of EDA-FN in response to treatment with TGF-β (Figure 9c and d). Therefore, EDA-FN does not appear to be responsible for the increased thickness of TGF-β-treated 3D ECM tissues, which suggests that alternative molecular mechanisms are responsible for this morphological transformation. Taken together, these results show that DFUFs respond differently to TGF-β stimulation than DFFs and NFFs, which may affect their ability to promote healthy wound healing.

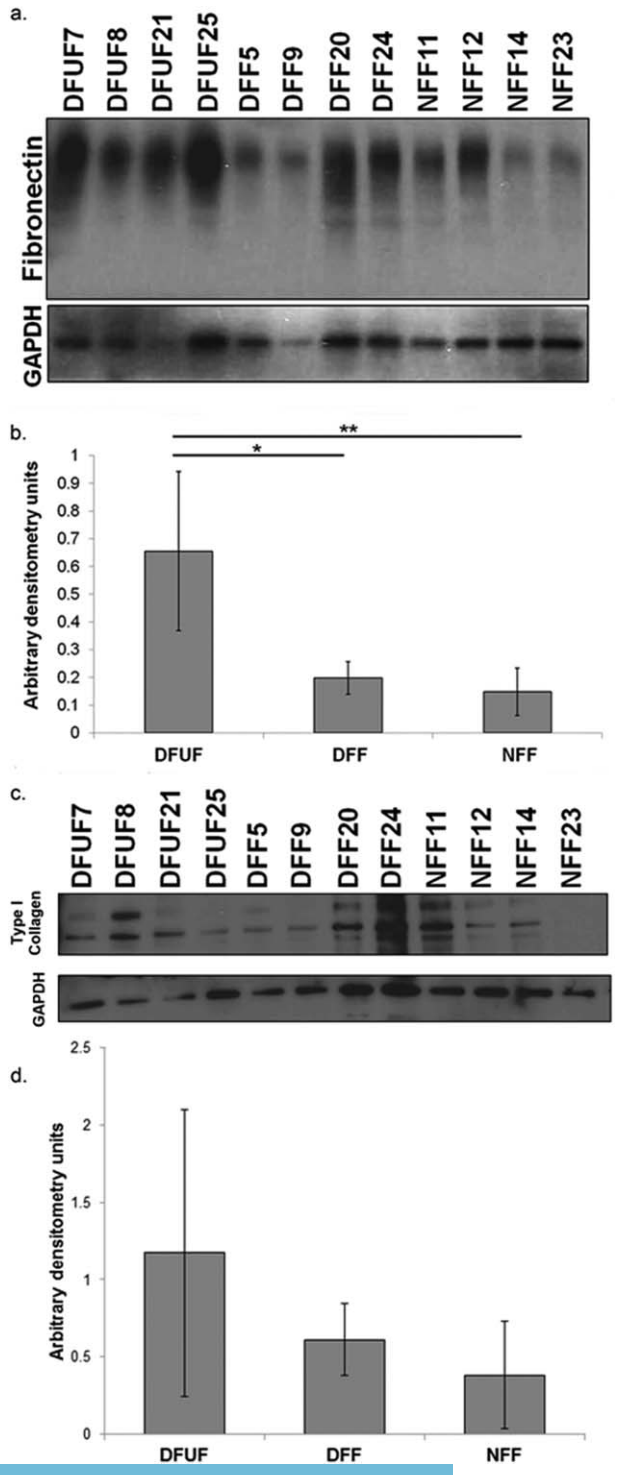

Figure 7. DFUF-produced 3D ECM tissues were enriched in fibronectin and Type I Collagen. (a) Western blots for fibronectin and loading control, GAPDH, are shown for protein extracted from 3D ECM tissues produced by DFUFs, DFFs and NFFs. (b) Densitometric quantification of fibronectin expression normalized to GAPDH and averaged for each fibroblast group revealed that DFUF-produced ECMs contain significantly more fibronectin than either DFF- or NFF-produced tissues. $*p \leq 0.05$, $**p \leq 0.01$. (c) Western blots show amounts of Type I Collagen normalized to GAPDH present in 3D ECM tissues produced by DFUFs, DFFs and NFFs. (d) Densitometric quantification of Type I Collagen expression normalized to GAPDH and averaged for each fibroblast group revealed that DFUF- and DFU-produced ECMs contain more Type I Collagen than NFF-produced tissue.

DISCUSSION

How ECM synthesis and assembly is altered in DFU-derived fibroblasts and the means by which it may impact chronic wound healing is poorly understood. In this study, we present findings using a group of primary,

www.manaraa.com

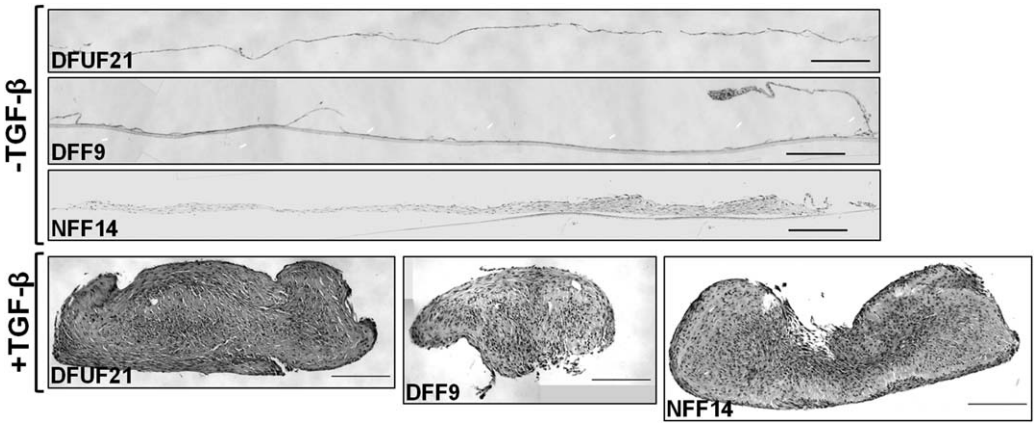

Figure 8. TGF-β treatment altered the morphology of 3D ECM tissues produced by DFUFs, DFFs, and NFFs. Self-assembled ECM tissues produced by DFUFs, DFFs, and NFFs were stimulated with TGF-β for 2 weeks. Images of H&E stained sections show that all three fibroblast types respond to TGF-β by altering their morphology; TGF-β-treated tissues were short and thick, untreated tissues were long and thin. Scale bar, 500 μM.

patient-derived DFU-derived fibroblasts and site-matched control fibroblasts. We show that DFU-derived fibroblasts produce and deposit an altered ECM that may have important functional consequences in the poor healing of chronic diabetic foot ulcers.

We first established the utility of these DFU-derived cells by confirming that fibroblast cell strains isolated from diabetic patients have overlapping patterns of gene expression that are distinct from fibroblasts isolated from healthy, control patients. Differential expression of diabetes and wound healing related genes confirmed that the primary fibroblasts retained relevant gene expression profiles during culture in vitro. While fibroblasts from venous ulcers, pressure ulcers, and DFUs have previously been isolated and cultured in monolayer[15,16,27,28] this is the first study to evaluate global gene expression differences in multiple, site-matched, patient-derived fibroblast strains. Thus, these primary, site-matched fibroblasts are a valuable resource for studying the properties of DFUs and diabetes in vitro.

We evaluated the functional translation of these gene expression differences in a 3D self-assembled ECM model that is more physiologically relevant than monolayer culture.[20,21] Using this 3D tissue model, we demonstrated that DFU-derived fibroblasts generated a thinner ECM compared to those generated by site-matched healthy fibroblasts, suggesting that the de novo production and assembly of ECM may contribute to the impaired healing of DFUs. Furthermore, the 3D ECM tissues generated by DFU-derived fibroblasts were enriched in the ECM protein, fibronectin. Sustained expression of fibronectin has previously been demonstrated in diabetic nephropathy,[19] however, its role in the pathogenesis of other diabetic complications, such as DFUs, remains unclear. It is known that fibronectin is the primary constituent of the provisional matrix following cutaneous wounding and provides a scaffold for collagen deposition and subsequent ECM remodeling.[17] However, in order for tissue repair to proceed properly, this fibronectin-rich matrix must be replaced by a more mature matrix.[6,29] Therefore, the prolonged and elevated expression of fibronectin in DFUs may limit the progression of normal wound healing. Yet, the role of fibronectin in stimulating wound repair is controversial, as it has been shown to both stimulate wound healing in normal[30] and diabetic wounds,[4] but also to limit regeneration.[6] Our finding supports that elevated fibronectin is a phenotype associated with poor wound healing in diabetic patients. Consequently, fibronectin may be an important target for DFU treatment; perhaps facilitating fibronectin clearance and the progression to a more mature matrix could enable tissue repair.[6]

Interestingly, we observed differences when comparing gene expression in monolayer cultures and 3D ECM tissue models. Also, NFF11 serves as an outlier with respect to gene expression and collagen immunoreactivity in 2D, however it appears to respond similarly to other NFF cultures in 3D. This suggests that more in vivo–like tissue models are useful in studying the complex cell behavior related to matrix deposition. Using the 3D ECM tissue model, we found that DFU-derived fibroblasts responded to TGF-β, contrary to previous evidence that chronic wound fibroblasts are unresponsive to stimulation by TGF-β. However, DFUFs failed to induce fibronectin expression in response to TGF-β, suggesting that abnormal growth factor response could contribute to the relative lack of success of growth factor therapies.

In summary, this work supports that DFU-derived fibroblasts contribute to impaired wound healing through aberrant ECM production and growth factor response. Our findings extend previous studies that have assessed ECM production in monolayer cultures by utilizing a more biologically relevant 3D tissue model.[3,31] Importantly, this study provides a strong rationale for the use of biomimetic tissue models that incorporate primary patient-derived cells to study complex cell behaviors and to more predicatively screen therapeutic agents targeting the chronic wound ECM.

www.manaraa.com

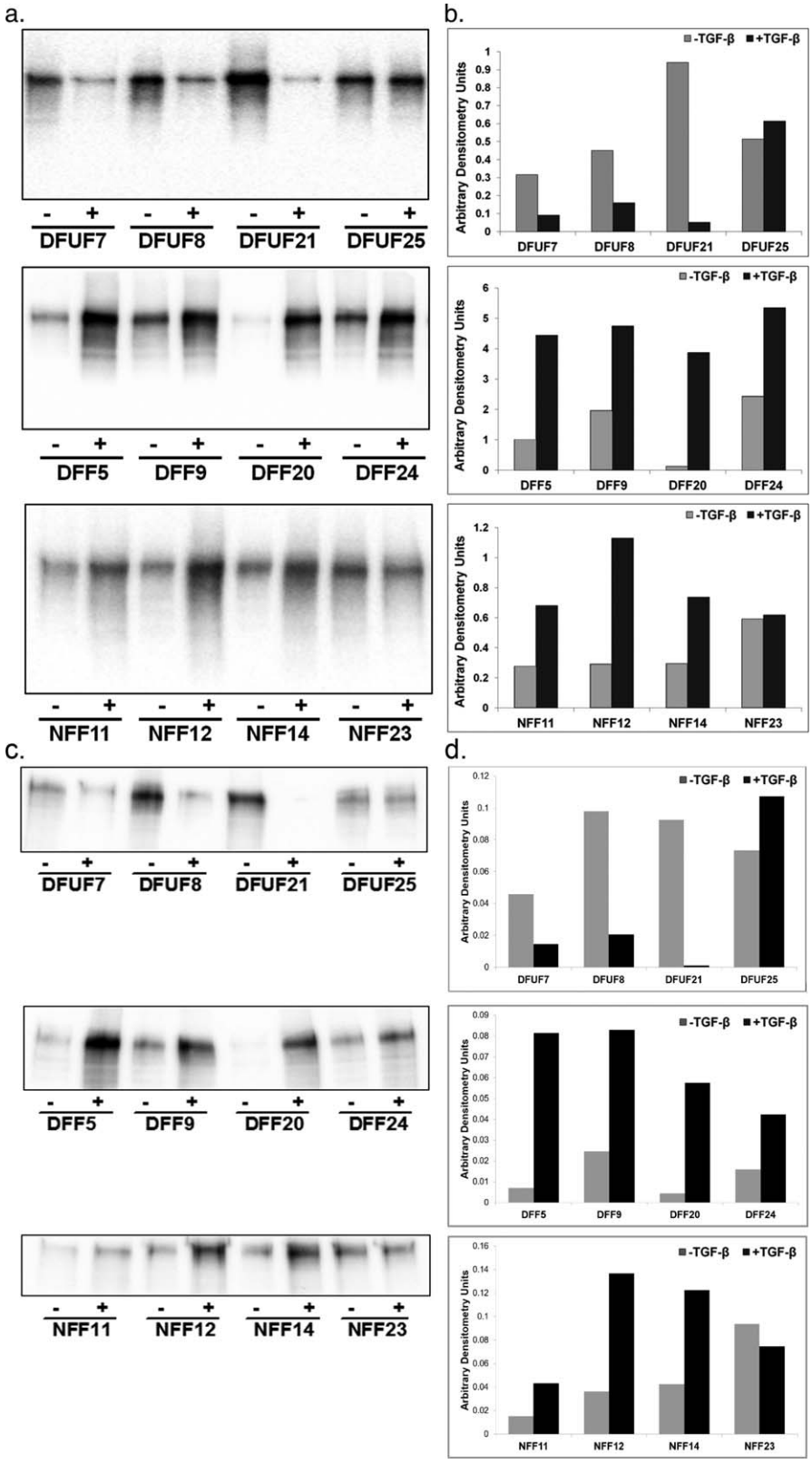

Figure 9. Aberrant production of fibronectin and EDA-containing fibronectin by DFUFs in response to TGF-β. (a) Western blot analysis of TGF-β stimulated ECM tissues produced by DFUFs, DFFs, and NFFs is shown. Fibronectin content was greater with TGF-β treatment in ECM tissues produced by all four DFFs and three of four NFFs. Conversely, fibronectin content was less with TGF-β treatment in ECM tissues produced by three of four DFUFs. (b) Densitometric quantification of fibronectin relative to total protein loaded confirms an altered response of DFUFs to TGF-β. (c) Western blot analysis of EDA-containing fibronectin amounts in TGF-β stimulated ECM tissues produced by DFUFs, DFFs, and NFFs is shown. EDA-containing fibronectin was increased by TGF- β stimulation in DFFs and NFFs. Conversely, in DFUFs TGF-β stimulation decreased the amount of EDA-containing fibronectin. (d) Densitometric quantification of EDA-containing fibronectin relative to total protein loaded confirms an altered response of DFUFs to TGF-β.

www.manaraa.com

ACKNOWLEDGMENTS

The authors would like to acknowledge J. Knowlton-Davis, G. Carpinito, J. Barretto, L. K. Park, and J. Edwards for their contributions and assistance.

Sources of Funding: This work was supported by grant #DK098055-06A1 to Jonathan A. Garlick from National Institute of Health (NIH).

Conflicts of Interest: No competing financial interests exist.

REFERENCES

1. Claudy AL, Mirshahi M, Soria C, Soria J. Detection of undegraded fibrin and tumor necrosis factor-alpha in venous leg ulcers. *J Am Acad Dermatol* 1991; 25: 623–7.
2. Falanga V. Chronic wounds: pathophysiologic and experimental considerations. *J Invest Dermatol* 1993; 100: 721–5.
3. Grinnell F, Ho CH, Wysocki A. Degradation of fibronectin and vitronectin in chronic wound fluid: analysis by cell blotting, immunoblotting, and cell adhesion assays. *J Invest Dermatol* 1992; 98: 410–6.
4. Hamed S, Ullmann Y, Egozi D, Daod E, Hellou E, Ashkar M, et al. Fibronectin potentiates topical erythropoietin-induced wound repair in diabetic mice. *J Invest Dermatol* 2011; 131: 1365–74.
5. Loots MA, Lamme EN, Zeegelaar J, Mekkes JR, Bos JD, Middelkoop E. Differences in cellular infiltrate and extracellular matrix of chronic diabetic and venous ulcers versus acute wounds. *J Invest Dermatol* 1998; 111: 850–7.
6. Stoffels JMJ, Zhao C, Baron W. Fibronectin in tissue regeneration: timely disassembly of the scaffold is necessary to complete the build. *Cell Mol Life Sci CMLS* 2013; 70: 4243–53.
7. Rosner K, Ross C, Karlsmark T, Petersen AA, Gottrup F, Vejlsgaard GL. Immunohistochemical characterization of the cutaneous cellular infiltrate in different areas of chronic leg ulcers. *APMIS Acta Pathol Microbiol Immunol Scand* 1995; 103: 293–9.
8. Herrick SE, Sloan P, McGurk M, Freak L, McCollum CN, Ferguson MW. Sequential changes in histologic pattern and extracellular matrix deposition during the healing of chronic venous ulcers. *Am J Pathol* 1992; 141: 1085–95.
9. Duraisamy Y, Slevin M, Smith N, Bailey J, Zweit J, Smith C, et al. Effect of glycation on basic fibroblast growth factor induced angiogenesis and activation of associated signal transduction pathways in vascular endothelial cells: possible relevance to wound healing in diabetes. *Angiogenesis* 2001; 4: 277–88.
10. Gurtner GC, Werner S, Barrandon Y, Longaker MT. Wound repair and regeneration. *Nature* 2008; 453: 314–21.
11. Stojadinovic O, Brem H, Vouthounis C, Lee B, Fallon J, Stallcup M, et al. Molecular pathogenesis of chronic wounds: the role of beta-catenin and c-myc in the inhibition of epithelialization and wound healing. *Am J Pathol* 2005; 167: 59–69.
12. Falanga V, Eaglstein WH, Bucalo B, Katz MH, Harris B, Carson P. Topical use of human recombinant epidermal growth factor (h-EGF) in venous ulcers. *J Dermatol Surg Oncol* 1992; 18: 604–6.
13. Ehrenreich M, Ruszczak Z. Update on tissue-engineered biological dressings. *Tissue Eng* 2006; 12: 2407–24.
14. Okiyama N, Kitajima T, Ito Y, Yokozeki H, Miyasaka N, Kohsaka H. Addition of the collagen binding domain of fibronectin potentiates the biochemical availability of hepatocyte growth factor for cutaneous wound healing. *J Dermatol Sci* 2011; 61: 215–7.
15. Herrick SE, Ireland GW, Simon D, McCollum CN, Ferguson MW. Venous ulcer fibroblasts compared with normal fibroblasts show differences in collagen but not fibronectin production under both normal and hypoxic conditions. *J Invest Dermatol* 1996; 106: 187–93.
16. Agren MS, Steenfos HH, Dabelsteen S, Hansen JB, Dabelsteen E. Proliferation and mitogenic response to PDGF-BB of fibroblasts isolated from chronic venous leg ulcers is ulcer-age dependent. *J Invest Dermatol* 1999; 112: 463–9.
17. Martin P. Wound healing–aiming for perfect skin regeneration. *Science* 1997; 276: 75–81.
18. Qiu Z, Kwon AH, Kamiyama Y. Effects of plasma fibronectin on the healing of full-thickness skin wounds in streptozotocin-induced diabetic rats. *J Surg Res* 2007; 138: 64–70.
19. Mason RM, Wahab NA. Extracellular matrix metabolism in diabetic nephropathy. *J Am Soc Nephrol* 2003; 14: 1358–73.
20. Maione AG, Brudno Y, Stojadinovic O, Park LK, Smith A, Tellechea A. Three-dimensional human tissue models that incorporate diabetic foot ulcer-derived fibroblasts mimic in vivo features of chronic wounds. *Tissue Eng Part C Methods* 2015; 21: 499–508.
21. Shamis Y, Hewitt KJ, Bear SE, Alt-Holland A, Qari H, Margvelashvilli M. iPSC-derived fibroblasts demonstrate augmented production and assembly of extracellular matrix proteins. *In Vitro Cell Dev Biol Anim* 2012; 48: 112–22.
22. Smyth GK. LIMMA: linear models for microarray data. In: Gentleman R, Carey V, Dudoit S, Irizarry R, Huber W (eds). *Bioinformatics and Computational Biology Solutions Using R and Bioconductor*. New York: Springer; 2005: 397–420.
23. Dai Y, Guo L, Li M, Chen YB. Microarray Я US: a user-friendly graphical interface to Bioconductor tools that enables accurate microarray data analysis and expedites comprehensive functional analysis of microarray results. *BMC Res Notes* 2012; 5: 282
24. Eden E, Navon R, Steinfeld I, Lipson D, Yakhini Z. GOrilla: a tool for discovery and visualization of enriched GO terms in ranked gene lists. *BMC Bioinformatics* 2009; 10: 48
25. Ngo P, Ramalingam P, Phillips JA, Furuta GT. Collagen gel contraction assay. *Methods Mol Biol Clifton NJ* 2006; 341: 103–9.
26. Park LK, Maione AG, Smith A, Gerami-Naini B, Iyer LK, Mooney DJ. Genome-wide DNA methylation analysis identifies a metabolic memory profile in patient-derived diabetic foot ulcer fibroblasts. *Epigenetics* 2014; 9: 1339–49.
27. Moor AN, Vachon DJ, Gould LJ. Proteolytic activity in wound fluids and tissues derived from chronic venous leg ulcers. *Wound Repair Regen Off Publ Wound Heal Soc Eur Tissue Repair Soc* 2009; 17: 832–9.
28. Hasan A, Murata H, Falabella A, Ochoa S, Zhou L, Badiavas E. Dermal fibroblasts from venous ulcers are unresponsive to the action of transforming growth factor-beta 1. *J Dermatol Sci* 1997; 16: 59–66.
29. Kishore R, Verma SK, Mackie AR, Vaughan EE, Abramova TV, Aiko I. Bone marrow progenitor cell therapy-mediated paracrine regulation of cardiac miRNA-155 modulates fibrotic response in diabetic hearts. *PloS One* 2013; 8: e60161
30. Martino MM, Tortelli F, Mochizuki M, Traub S, Ben-David D, Kuhn GA. Engineering the growth factor microenvironment with fibronectin domains to promote wound and bone tissue healing. *Sci Transl Med* 2011; 3: 100ra89

www.manaraa.com

31. Stephens P, Davies KJ, al-Khateeb T, Shepherd JP, Thomas DW. A comparison of the ability of intra-oral and extra-oral fibroblasts to stimulate extracellular matrix reorganization in a model of wound contraction. *J Dent Res* 1996; 75: 1358–64.

Supporting Information

Additional Supporting Information may be found in the online version of this article at the publisher's web-site:

Figure S1. TGF-β treatment increased fibronectin expression. Monolayer cultures of DFUFs, DFFs, and NFFs were treated for 48 hours with 2 ng/mL TGF-β or vehicle control and stained for fibronectin and DAPI. TGF-β treatment resulted in an increase in fibronectin staining over vehicle control treatment. No significant staining differences were observed between DFUFs, DFFs, and NFFs, though there was a slight trend towards less fibronectin expression by DFUFs. Since staining was similar within fibroblast groups, only one representative fibroblast strain is shown per group.

Figure S2. DFUFs failed to contract collagen gels in response to TGF-β stimulation. Collagen gels populated with DFUFs, DFFs, or NFFs were treated with 2 ng/mL TGF-β or vehicle control for five days. Quantification of mean ± S.D. percent reduction in surface area relative to vehicle control treatment for each fibroblast group is shown. DFFs and NFFs increased gel contraction in response to TGF-β treatment, while DFUFs failed to promote contraction with TGF-β stimulation. *$P \leq 0.05$.

Table S1. Primers sequences.

Table S2. DFUF vs. NFF differentially expressed genes.

Table S3. DFF vs. NFF differentially expressed genes.

Table S4. DFUF vs. DFF differentially expressed genes.

www.manaraa.com

Copyright of Wound Repair & Regeneration is the property of Wiley-Blackwell and its content may not be copied or emailed to multiple sites or posted to a listserv without the copyright holder's express written permission. However, users may print, download, or email articles for individual use.

www.manaraa.com